

AD _____

AWARD NUMBER DAMD17-96-1-6139

TITLE: X-Photon-to-Information Conversion Efficiency in Digital
Telemammography

PRINCIPAL INVESTIGATOR: Celeste B. Williams

CONTRACTING ORGANIZATION: Ohio State University
Columbus, Ohio 43210

REPORT DATE: June 1998

TYPE OF REPORT: Annual

PREPARED FOR: Commander
U.S. Army Medical Research and Materiel Command
Fort Detrick, Maryland 21702-5012

DISTRIBUTION STATEMENT: Approved for public release;
distribution unlimited

The views, opinions and/or findings contained in this report are those of the author(s) and should not be construed as an official Department of the Army position, policy or decision unless so designated by other documentation.

DRG QUALITY INSPECTED 1

19980917 013

REPORT DOCUMENTATION PAGE

Form Approved
OMB No. 0704-0188

Public reporting burden for this collection of information is estimated to average 1 hour per response, including the time for reviewing instructions, searching existing data sources, gathering and maintaining the data needed, and completing and reviewing the collection of information. Send comments regarding this burden estimate or any other aspect of this collection of information, including suggestions for reducing this burden, to Washington Headquarters Services, Directorate for Information Operations and Reports, 1215 Jefferson Davis Highway, Suite 1204, Arlington, VA 22202-4302, and to the Office of Management and Budget, Paperwork Reduction Project (0704-0188), Washington, DC 20503.

1. AGENCY USE ONLY (Leave blank)		2. REPORT DATE June 1998	3. REPORT TYPE AND DATES COVERED Annual (1 Jun 97 - 31 May 98)	
4. TITLE AND SUBTITLE X-Photon-to-Information Conversion Efficiency in Digital Telemammography			5. FUNDING NUMBERS DAMD17-96-1-6139	
6. AUTHOR(S) Celeste B. Williams				
7. PERFORMING ORGANIZATION NAME(S) AND ADDRESS(ES) Ohio State University Columbus, Ohio 43210			8. PERFORMING ORGANIZATION REPORT NUMBER	
9. SPONSORING / MONITORING AGENCY NAME(S) AND ADDRESS(ES) U.S. Army Medical Research and Materiel Command Fort Detrick, Maryland 21702-5012			10. SPONSORING / MONITORING AGENCY REPORT NUMBER	
11. SUPPLEMENTARY NOTES				
12a. DISTRIBUTION / AVAILABILITY STATEMENT Approved for Public Release; Distribution Unlimited			12b. DISTRIBUTION CODE	
13. ABSTRACT (Maximum 200 words) The objective of our study is to noninvasively characterize the mechanical properties of normal breast tissue to use in realistic tissue modeling for medical visualization and simulation. Primary aspects of the research emphasize the mechanical deformation of normal breast tissue subjected to incremental compressive forces, and the investigation and implementation of computer algorithms for image morphing and 3D visualization. With the biomechanical principles of breast tissue, we propose to develop a biomechanically driven computer morphing algorithm that accurately mimics the shape deformation of normal breast tissue. In our investigations, we found that MR imaging can provide <i>in vivo</i> biomechanical information about the breast, as well as provide 3D data sets for volume visualization.				
14. SUBJECT TERMS Breast Cancer			15. NUMBER OF PAGES 36	
			16. PRICE CODE	
17. SECURITY CLASSIFICATION OF REPORT Unclassified	18. SECURITY CLASSIFICATION OF THIS PAGE Unclassified	19. SECURITY CLASSIFICATION OF ABSTRACT Unclassified	20. LIMITATION OF ABSTRACT Unlimited	

FOREWORD

Opinions, interpretations, conclusions and recommendations are those of the author and are not necessarily endorsed by the U.S. Army.

_____ Where copyrighted material is quoted, permission has been obtained to use such material.

_____ Where material from documents designated for limited distribution is quoted, permission has been obtained to use the material.

_____ Citations of commercial organizations and trade names in this report do not constitute an official Department of Army endorsement or approval of the products or services of these organizations.

_____ In conducting research using animals, the investigator(s) adhered to the "Guide for the Care and Use of Laboratory Animals," prepared by the Committee on Care and Use of Laboratory Animals of the Institute of Laboratory Resources, National Research Council (NIH Publication No. 86-23, Revised 1985).

_____ For the protection of human subjects, the investigator(s) adhered to policies of applicable Federal Law 45 CFR 46.

_____ In conducting research utilizing recombinant DNA technology, the investigator(s) adhered to current guidelines promulgated by the National Institutes of Health.

_____ In the conduct of research utilizing recombinant DNA, the investigator(s) adhered to the NIH Guidelines for Research Involving Recombinant DNA Molecules.

_____ In the conduct of research involving hazardous organisms, the investigator(s) adhered to the CDC-NIH Guide for Biosafety in Microbiological and Biomedical Laboratories.

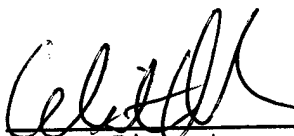
 6/28/98
PI - Signature Date

TABLE OF CONTENTS

I. Standard Form (SF) 298

II. Foreword

III. Introduction

A. Background

a. Mechanical Deformation

b. Initial Morphing Algorithms

VI. Body of Report

A. Methods

B. Results and Discussion

a. Stress Sensors

b. Surface Coil

1. Correction Algorithm

2. *In Vivo* Landmarks

c. Tissue Deformation

1. Deformation Calculations

d. Morphing Algorithms

1. 2D Morphing

2. 3D Morphing

e. Significance

V. Conclusion

VI. References

VII. Appendices

INTRODUCTION

Presently, the imaging techniques used for diagnosis and detection of breast cancer are all performed by deforming the breast from its original shape. These shape deformations result in improved diagnostic image quality, however, the biomechanical nature of breast tissue is not taken into account. This is largely due to the fact that the biomechanical behavior of breast tissue is not fully understood. An understanding of the biomechanical properties of breast tissue may aid the development of accurate breast models, and the characterization of the mechanical nature of tissue may provide diagnostic information.

The purpose of our study is to noninvasively characterize the mechanical properties of normal breast tissue, and to develop a biomechanically driven computer morphing algorithm that accurately mimics the shape deformation of normal breast tissue.

This report describes present research and tasks completed according to the BAA proposal. As outlined in the Statement of Work, the main objectives of the second year of research are:

- A. The design and development of a MR compatible compression device.
- B. Investigation of morphing algorithms.

With the design and development of the MR compatible compression device completed, studies of the mechanical deformation of normal breast tissue are underway, and considerable progress has been made with the investigation and implementation of computer algorithms for image morphing and 3D visualization.

BACKGROUND

Mechanical Deformation

The biomechanical nature of soft tissue is described in terms of its stress - strain or constitutive relationship. Strain is a measurement of the deformation or displacement of a material caused by the stress, and stress equals force per unit area of contact. The particular shape of the deformation is a function of both the internal strains and stresses within the tissue, and the external forces applied to the tissue.

The breast is a composite of mechanically different materials. It is considered as a mixture of a porous matrix in an incompressible fluid. The ductal system comprises about 10-15% of the total breast mass. The remaining 85% is mostly adipose tissue [1]. Both adipose and glandular tissues obtain their elasticity from elastic fibers. Breast tissue, like most soft tissue, is modeled as a non-linear, anisotropic, incompressible continuum [2]. The action of external forces causes deformation and a change of internal (potential) energy. The elastic deformation of tissue is associated with this change of potential energy [3,4,5].

Provided that no energy is lost due to heat, the external work done by loads is converted into internal work, called strain energy. This energy is caused by the action of either normal or shear stress. If a cubic volume element is subjected to a compressive force normal to the top and bottom of the cubic faces in the z-direction, the force created on the top and bottom of the faces is

$$dF_Z = \sigma_Z dA \quad (1)$$

where A is the surface area of the cubic face, F_Z is the applied force, and σ_Z is the normal stress. If the force is applied gradually, as in static loading, the volume element undergoes a displacement in the Z-direction of

$$d\Delta Z = \varepsilon_Z dZ, \quad (2)$$

where $\Delta Z = Z_0 - Z$ and ε_Z is the strain. Z_0 is the original length, and Z is the deformed length. The work done by the force is therefore,

$$\begin{aligned} dU &= \frac{1}{2} dF_Z d\Delta Z \\ &= \frac{1}{2} (\sigma_Z dX dY) \varepsilon_Z dZ \\ &= \frac{1}{2} \sigma_Z \varepsilon_Z dV \end{aligned} \quad (3)$$

where $dV = dX dY dZ$.

The strain energy density function can serve as the constitutive equation to relate stress to strain. The strain energy function is a function of the strain components and depends on the invariants of the strain and thus states the isotropic nature of materials.

$$U = U(I_1, I_2, I_3) \quad (4)$$

where U is the energy density function, and I_1, I_2, I_3 are the strain invariants. For incompressible materials, $I_3 = 0$ and the strain energy relation has the form [5,6],

$$U = C_0(I_1 - 3) + C_1(I_2 - 3) \quad (5)$$

where C_0 and C_1 are constants. A major constraint for modeling of breast tissue is that the model correctly represents the deformability of real tissue. In order to control the accuracy of the deformation model, we have proposed to compare the computed deformation of the soft tissue with the actually deformed tissue.

Initial Morphing Algorithms

Image morphing is useful in displaying deformation because the displacements can be smooth from one position to another. Control points such as in finite element models may be warped and morphed. Points and lines guide the morphing process, and when the control points are warped, deformation of the material is generated. While existing computer algorithms can efficiently simulate deformation, they largely ignore the physical principles of deformation. These computer algorithms use geometric primitives such as triangles to compute deformations.

Finite element models are the most widely employed deformable tissue models used because they can model a continuum. The finite element method describes a volume or surface as a set of basic elements, such as tetrahedra, triangles, and other polygons. Splines can be seen as finite elements with a definite shape function. Spline interpolation represents a type of mesh deformation model whereby application of moving groups of control points generates deformation [7].

A simple morphing algorithm commonly used is Free Form Deformation (FFD) in which point features are organized on a rectilinear mesh. In FFD, each deformation is associated with a deformation parallelepiped box. The points of the face of the box are expressed in the coordinate system of the box. The positions of the points are updated when the coordinates of the box are displaced.

Another morphing algorithm, known as Feature-Based Morphing, uses both points and lines as features. The defined control points and lines drive the displacements by using such factors as the distance to the nearest line segment and the length of the nearest line segment. As the number of control points increases, the more accurate the generated morph becomes [8].

A major problem of image morphing is foldover. If many-to-one correspondences occur between the source and the target at some point during a morph, then the resulting morph contains undesirable wrinkles or distortions in the images. When feature movements are small, most existing morphing algorithms can produce one-to-one mapping. However for large displacements, foldover can occur. The foldover-free technique constructs a triangulation over a given set of features. As the features move, the triangulation changes its structure and no edges in the triangulation may cross line features [8].

BODY OF REPORT

METHODS

Deformation information was obtained *in vivo* using magnetic resonance imaging to detect displacement of regions of interest, (i.e., landmarks). Imaging was performed on a GE 1.5 T clinical MR system (General Electric, Signa). Optimal fat and gland contrast was obtained by employing a spoiled gradient echo (SPGR) sequence. With a 3D imaging protocol, high signal-to-noise ratio (SNR) images were acquired. The protocol employs a fast 3D-FSPGR (fast spoiled gradient echo) sequence, with TE= 4.2 msec fat/water in-phase, TR=25 msec, flip angle = 60 degrees, a 512 x 256 matrix and field of view=20x20 cm². One hundred twenty-four 1.4 mm coronal slices were obtained for each compression. Acquisition times ranged from 4.50 to 8.12 minutes.

Initially, compression studies were performed with a commercial breast coil. In these studies the left breast was compressed with Pyrex plates in the cranial-to-caudal and medial-to-lateral directions. Because of the curvature of the breast coil, it was difficult to compress in the C-C position, however large local deformations were clearly visible in the M-L compression images. With the commercial breast coil, it was also difficult to supply incremental compressive loadings. Because of these findings, it was decided to image with flat surface coils. Although flat surface coils are known to produce spatial intensity variations, which can complicate image segmentation and visualization, the improved control of incremental changes in compression was found to be necessary for the proposed work. We therefore designed a combined coil-compression device for studying breast deformation.

The coil-compression device, shown in figure 1, consists of both a compression plate and a flat surface coil. The top compression plate moves vertically along posts to supply a uniaxial compression force, and the imaging coil is attached to the bottom plate. Mechanical stops control the compression and width. The compression plate is positioned on the breast to be imaged, with its edge against the rib cage. The movable plate pushes lightly into the chest wall and separates the left breast from the right breast to allow full coverage of only one breast. The compression plates contain a series of registration markings to provide localization landmarks. The subject lies on her side with the upper body slightly elevated. As shown in figure 1b, the surface coil is placed so that it rests up against the side of the chest wall beneath the breast, and the breast lies close to the surface coil. Most subjects reported this position as comfortable.

Uncompressed and compressed images of several healthy female volunteers, over the age of 18 and pre-menopausal were acquired. The breast was slightly compressed in the medial-lateral orientation with an uniaxial compression force. In this configuration, displacement and normal stresses may be experimentally evaluated. To measure the normal stress at specified landmarks, various force sensors were investigated. Versatile and economic sensors were required because an array of sensors had to be capable of being placed into the imaging magnet without introducing large artifacts.

RESULTS AND DISCUSSION

Stress Sensors

Traditional load cells used to measure force are metallic, inflexible and costly. The miniature load cells can cost as much as \$1,000 each. Therefore, we plan to measure normal stress with the non-metallic Uniforce[®] sensor. The sensor is constructed of two layers of non-conductive substrate with layers of a silver conductive material applied to each substrate. Force can be measured by connecting the sensor leads to an ohmmeter and measuring the change in resistance. There is also software available that is capable of displaying the output of the sensor in units of pounds or newtons. The sensors are flexible, thin, about 0.076 mm, and capable of detecting static forces over a broad range. The thinness, flexibility, and cost of the sensors permit an array of the force sensors to be assembled and placed between the compression plate and the breast.

Several studies were conducted to evaluate if the sensors and connecting cables can be safely used in conjunction with MRI. Two main issues that needed to be addressed are:

- (1) Alternating magnetic fields may produce currents and potentially harmful heating leading to skin burns.
- (2) Presence of conductors may lead to imaging artifacts.

To address the safety concern, tests were conducted with two sensors taped to the hand of a subject. The subject's hand was placed inside a head coil and imaged for up to 6 minutes. The subject indicated no sense of increased temperatures near the sensors, and no heat burns were observed.

To address the conductivity issue, sensors with and without the connector assembly were attached to a gelatin phantom and imaged. For the sensor without the connector assembly, small susceptibility effects leading to signal voids of a few millimeters are observed. These tests indicate the possibility of using the sensor array as external landmarks.

For sensors with the connector assembly, 2 x 2 cm signal voids are found. We concluded that for the *in vivo* stress studies, the sensor connectors must be at least 2 cm away from the breast.

Surface Coils

From the MR images acquired using a flat surface coil, anatomical features are clearly identifiable and noise due to respiratory and cardiac motion is minimal, although some aliasing is observed. Chemical shift at tissue boundaries in the frequency encode direction is also observed, but does not appear to be prohibitive.

Correction Algorithms:

One problem with using the flat surface coil is signal drop-off. The inhomogeneous sensitivity profile of the coil produces intensity variations that spatially lower contrast and limit optimal display. Because signal intensity varies across the width of the coil, some anatomical features are not clearly distinguishable on images. Furthermore, the large signal variation is prohibitive for the planned computer processing. Signal correction is possible by dividing out the transfer function of the coil [9].

$$\text{Corrected image} = \text{original image} / h_{cp}$$

where h_{cp} is the estimated surface coil's sensitivity profile. Initially a low pass filtering technique was used to estimate h_{cp} . [9]. As shown in figure 2, with this correction method some signal correction is observed but the contrast is still low. This method also introduces additional noise into the image.

A better correction technique was developed to correct the surface coil images and increase tissue contrast. The new method uses a homogeneous phantom and patented external markers [10]. External registration markers are placed on the plates of the compression device and the h_{cp} is found from a uniform gelatin phantom.

$$\text{Phantom image} = h_{cp}$$

The phantom images are smoothed with an averaging filter to reduce noise, and the images of the breast and the phantom are aligned section by section using the external markers. An example of the image correction with this new method is shown in figure 3.

In Vivo Landmarks:

From preliminary imaging outlined in the 1997 Annual Report, anatomical features such as the rib cage, branching ducts, fatty tissue, boundaries between glandular and fatty tissue and the nipple are clearly visible on MR images. With the correction method described above, segmentation of these anatomical features is easily accomplished. However, automatically segmenting adipose tissue from the branching ducts remains a problem to be addressed. Anatomical features serve as positional markers of tissue deformation, and are used as landmarks to define the control points for the morphing algorithms. The three principle types of landmarks characterized are: 1). points at which two or more structures meet, 2). tips of extrusions, and 3). tangential points along curved surfaces.

Tissue Deformation

The mechanical behavior of breast tissue is clearly represented on the sectional MR images. Substantial tissue deformations are observed even under the mildest of compression. Figure 4a demonstrates in sections near the nipple where compression is the least, the tissue appears to have rotated. This rotation is observed in most subjects. This specific type of deformation is assumed to be associated with compression in the medial-lateral orientation. Future studies will also include cranial-to-caudal compression. Shown in figure 4b are MR sections closer to the chest wall, where tissue deformation is clearly distinguishable.

Deformation Calculations:

Using the mechanical stops to control the distance between the top compression plate and the bottom plate, subjects were imaged with a range of compressions. The right breast was compressed in the medial-lateral direction and widths and percent of deformation of the breast are given in Table 1.

TABLE 1. Percent compression in the direction of the applied force.

	subject 1	subject 2	subject 3	subject 4
uncompressed width	100	77	55	75
(mm)				
compressed width	80	57	35	55
(mm)				
% deformation in Z direction	20.0	26.0	36.4	26.7

Table 2 displays the deformation calculated for a small volume of tissue using the center MR sections of compressed and uncompressed breast tissue. The displacement vector represents the displacement of a point P, located at x, y, z in the original volume, to the displaced point P', located at x', y', z' in the deformed volume. The coordinate system is defined such that the plates compress in the Z-direction (right to left orientation). The X-axis is in the subject's inferior to superior direction, and the Y-axis points from the nipple to the chest wall (anterior to posterior direction),(see figure 1b).

TABLE 2. Components of the displacement vector of specific landmarks undergoing an applied compressive force.

	X-direction	Y-direction	Z-direction
P1	0.436	0.542	0.719
P2	0.251	0.292	0.923
P3	0.093	0.317	-0.944
P4	-0.990	0.090	-0.104
P5	-0.005	-0.988	0.151
P6	0.200	-0.978	-0.065
P7	0.173	-0.969	-0.175
P8	0.159	-0.984	0.074

Along the Z-axis, the minus sign represents displacement opposite to the direction of the applied compression force. Along the X and Y axes, the minus sign represents displacement that increases from an arbitrarily chosen origin. Points P1-P3 are the farthest away from the compression plate and the largest displacements are observed along the Z-axis in the direction of compression. In these sections, some shear displacements are observed in the X and Y directions. This supports the observation of tissue rotation in MR sections near the nipple.

The largest displacements are along the Y axis for points closer to the chest wall and to the compression plate, (points P6-P8). This is because in medial-lateral compression, the stress is greater near the chest wall than near the nipple, and the deformation in the Y direction is elongated. Even for small compressions with the breast compressed <20%, the out-of-plane elongation can be large.

Morphing Algorithms

2D Morphing:

We began our study by investigating two-dimensional image processing because of the abundance of literature and availability of techniques in 2D morphing. Several computer morphing techniques such as Free Form Deformation (FFD) and feature-based morphing have been investigated. The 2D morphing gives favorable results with the computer algorithm yielding a morphed image that is similar to the target image. The algorithms map landmarks from the source image to the target image. Control points are chosen according to the internal and external landmark studies discussed in last year's report.

In the preliminary study, a 2D FFD computer morphing algorithm was employed to map internal anatomical landmarks from prone breast images obtained with a commercial breast coil (the

source image), to supine breast images obtained with a body coil (the target image). The prone images have high resolution, but the supine images are noisy because they were acquired with the body coil and due to cardiac and respiratory motion, (see figure 5).

Image control features that guide the morphing process are shown in figure 5a. Point and line features in figure 5a are drawn at locations classified as Type 2 and 3 landmarks. The generated morph shown in figure 6a is less noisy than the original supine image, however some areas of the generated supine image are not correctly morphed using the feature based algorithm.

A 2D Foldover-Free algorithm provides better one-to-one mapping and generates a better image, as shown in figure 7b. The prone to supine images exhibit very large deformations and provide little mechanical information. To better evaluate the mechanical properties of breast tissue, incremental deformations are required.

By applying static compression forces in small incremental steps, small deformations are obtained. The compressed and uncompressed images are shown in figure 8. Another 2D feature based morphing algorithm was employed on these images with image features controlling the morphing process. The point and line anatomical features in figure 8a are drawn at locations classified as Type 2 and 3 landmarks. For the morphing process, the uncompressed image is the source image (e.g., the beginning of the morphing process) and the compressed image is the target for the end of the morphing process.

The generated morphs are shown in figure 9. Some areas of the target image are not correctly morphed. As more control points are defined, a better image is generated and the correlation between the morph and target improves.

When feature movement or shape deformation is small, most morphing algorithms can produce a one-to-one mapping between source and target. For large deformations, however, overlapping between control points can occur. The Foldover-Free algorithm can provide better one-to-one mapping, eliminate overlap, and generate a better image. Such a 3D algorithm is currently under investigation for volume morphing [8].

3D Morphing:

Our initial data indicate that tissue deformation occurs in three dimensions. Thus, evaluations of breast biomechanics will have to be in 3D. Three-dimensional volume visualization is necessary to identify landmarks in 3D. We employed interactive volume visualization techniques for our 3D-MR data sets. Although volume based morphing techniques are not as widely available as 2D morphing, they are more suitable for 3D data because 2D morphing cannot display out of plane deformations.

Several methods of 3D visualization were investigated to determine which technique would best represent the tissue volume. The image in figure 10a displays a sagittal section of the entire breast obtained with a ray casting volume rendering technique. Although this representation is a

good 3D display of volume, it is not found to be appropriate for image morphing because it does not display out of plane branching of the ductal systems.

Our next step was to segment the volumetric MR data sets with appropriate thresholding to produce 3D representation of breast tissue. Figure 10b shows coronal sections of compressed and uncompressed 3D views of segmented data. This volume rendering is performed with a ray casting technique [11]. With this method, the tissue is too dense to adequately locate landmarks, although some extrusion peaks are displayed. Figure 11 shows a polygon rendering of sections of tissue in which the volumes are displayed as isosurfaces using the Marching Cubes Algorithm [11]. This rendering is the best 3D rendering obtained thus far. The out of plane branching of the ductal system is clearly represented in these images.

As can be seen from the images, identifying appropriate 3D landmark features from the segmented data to drive the morphing algorithm is a challenge. To perform 3D morphing, appropriate features that could be mapped to the target image are required. Type 2 landmarks (i.e., extrusion peaks) are favored because they are easier to identify. Slice by slice 2D morphing of the volume data can be easily accomplished, but 3D morphing is more problematic. A Mesh Free Form Deformation algorithm has been utilized for preliminary studies. In an MFFD algorithm the object is not deformed directly, but it is embedded in a space that is deformed. The effects of deforming that space are propagated to the object, (see figure 12b).

Significance

All objectives of the proposed research are on track and proceeding as scheduled. Tasks one, two, and three have been completed and tasks four and five have been initiated.

TASK 1: Investigate MR-visible materials. Characterize internal landmarks using anatomy of breast.

TASK 2: Identify internal and external MR visible markers. Investigate optimal MR imaging protocols. Identify breast models.

TASK 3: Investigate morphing algorithms to optimize MR localization using compressional and gravitational forces. Develop MR compression device.

TASK 4: Investigate morphing algorithms. Finite element methods and thin plate splines, FFD, and volume morphing.

TASK 5: Acquire deformation data. Estimate stress. Develop constitutive relationship.

The results of this work have been presented at Ohio State University, ISMRM, and BMES. A list of publications and presentations resulting from this work is included in the Appendices.

One notable outcome of our investigations is the surface coil intensity correction algorithm. We improved upon one existing algorithm to get more appropriate results. These findings will be published at a later date [12].

In keeping with the goals outlined in the Statement of Work, our next research steps are to:

- Focus on incremental compression to obtain small deformations
- Estimate the *in vivo* stress from the deformation data
- Measure the normal stress
- Implement 2D algorithms with tissue biomechanical properties

Because 2D computer morphing algorithms are available, we will continue with these algorithms and the constitutive relationship, using stress and strain vectors instead of 3 x 3 stress and strain tensors. This approach will simplify initial implementation of mechanical computation and use of mechanical information for morphing algorithms.

CONCLUSIONS

Localization of internal anatomy has been very promising using the internal and external landmarks. From the initial deformation data, we found that MR imaging can provide *in vivo* biomechanical information about the breast when incremental compression is used. We observed that because of the connectivity of the duct system, shear deformation occurs at regions far from the point of contact of the applied force. From the force sensors, measurements of the normal stress during compression deformation will be obtained, and with the estimates of *in vivo* stress and strain, the mechanical constitutive relationship of breast tissue can be approximated.

While computer morphing has proven beneficial in 2D morphing, a problem still exists for 3D morphing. As can be observed in the 3D volumes, it is difficult to identify enough point and line features to control the morphing process. This problem may be addressed by employing geometric solids to display the volume, and using physically based control systems instead of triangulation to represent the deformation. Such techniques have been employed for muscle deformation [13].

REFERENCES

1. Slauson, D. and Cooper, B., Mechanisms of Disease, Williams & Wilkins, Baltimore, 1990.
2. Fung, Y.C., Biomechanics: Mechanical Properties of Living Tissues. Springer-Verlag, New York, 1993.
3. Gallagher, R., Simon, B., Johnson, P., Gross, J., Finite Elements in Biomechanics, Wiley & Sons, New York, 1982.
4. Park, J., Lakes, R., Biomaterials, An Introduction, Plenum Press, New York, 1992.
5. Sumi, C., Suzuki, A., Nakayama, K., "Estimation of Shear Modulus Distribution in Soft Tissue from Strain Distribution", IEEE Transactions on Biomedical Engineering, Vol. 2, No.2, pp.193-204, 1995.
6. Humphrey, J.D., Yin, F.C.P., "On Constitutive Relations and Finite Deformations of Passive Cardiac Tissue: I. A pseudo strain-energy function", Journal of Biomechanical Engineering, Vol.100, pp.299-304, 1993.
7. Delingette, H., "Toward Realistic Soft-Tissue Modeling in Medical Simulation", Proceedings of the IEEE, Vol. 86, No.3, March, pp. 512-523, 1998.
8. Fujimura, K., Makarov, M., "Foldover-Free Image Warping", SIGGRAPH, December 1997.
9. Murakami, J., Hayes, C., Weinberger, E., "Intensity Correction of Phased-Array Surface Coil Images." Magnetic Resonance in Medicine, Vol.35, pp. 585-590, 1996.
10. Chakeres, D., Schmalbrock, P., Clymer, B., Deak, G., **Williams, C.**, "Multi-Vector Real Time Disposable Stereotactic MR Breast Biopsy System", submitted to Radiological Society of North America, 84th Scientific Assembly and Annual Meeting, 1998.
11. Schroeder, W., Martin K., Lorensen, B., The Visualization Toolkit, Prentice Hall, New Jersey, 1998
12. Chakeres, D., Schmalbrock, P., Clymer, B., Deak, G., **Williams, C.**, "MR Surface Coil Image Correction Using an Integrated Positional Reference System", submitted to Radiological Society of North America, 84th Scientific Assembly and Annual Meeting, 1998.
13. Ng-Thow-Hing, V., Fiume, E., "Interactive Display and Animation of B-Spline Solids as Muscle Shape Primitives," University of Toronto, Dynamics Graphics Project. 1998.

APPENDICES

a. Acronyms and Symbols

T - tesla

TR - repetition time

TE - echo time

T1- spin-lattice relaxation time of the magnetization along the longitudinal axis

T2- spin-spin relaxation time of magnetization in the transverse plane.

msec - millisecond

mm - millimeter

SNR - signal-to-noise ratio

SPGR- spoiled gradient echo

2D - two dimensional

3D - three dimensional

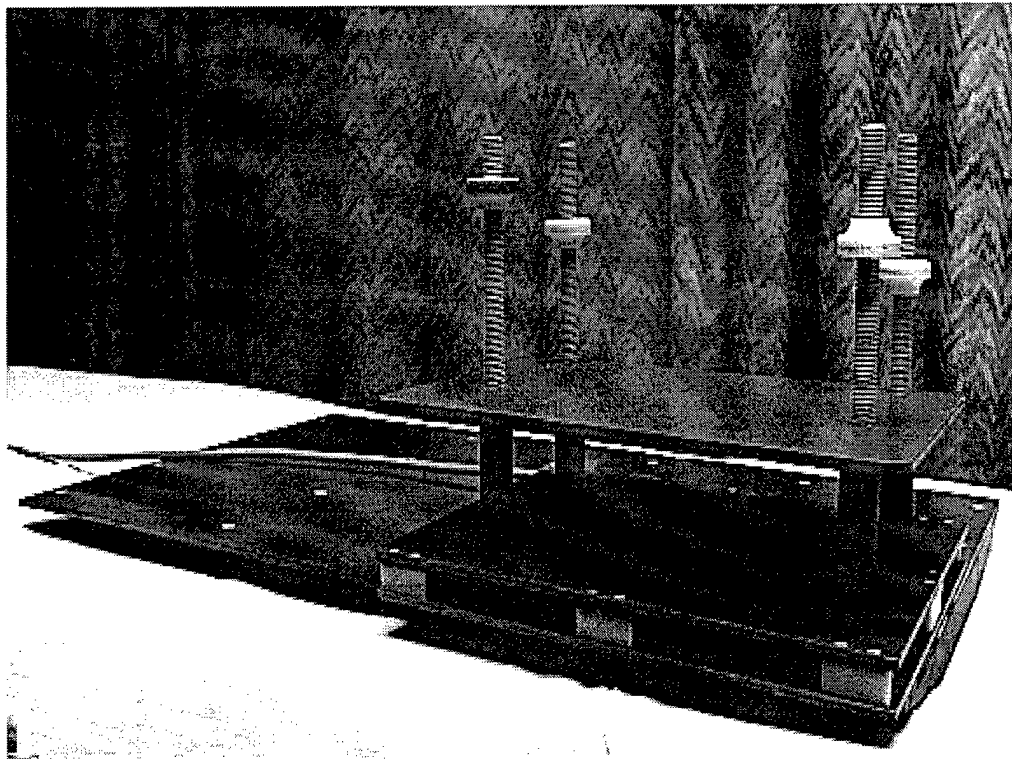
h_{cp} - coil's sensitivity profile

C-C - cranio-caudal

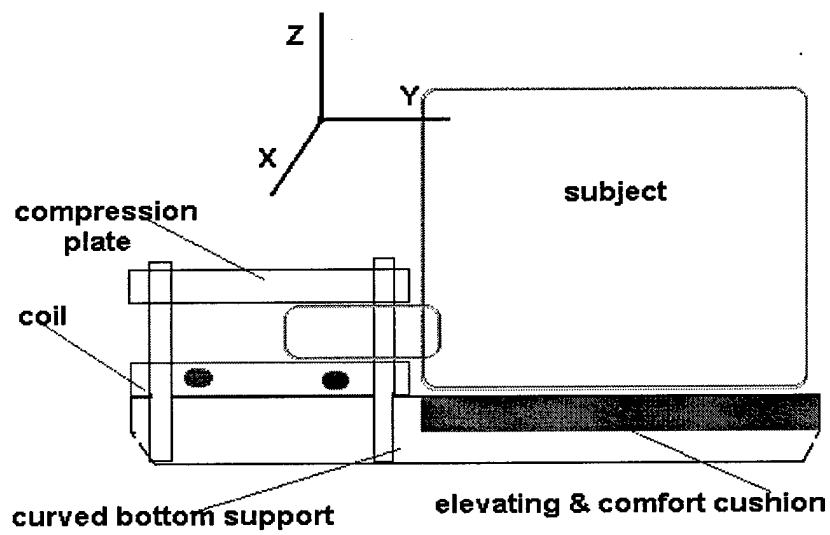
M-L - medio-lateral

deformation - $Z_0 - Z / Z_0$

b. Figures

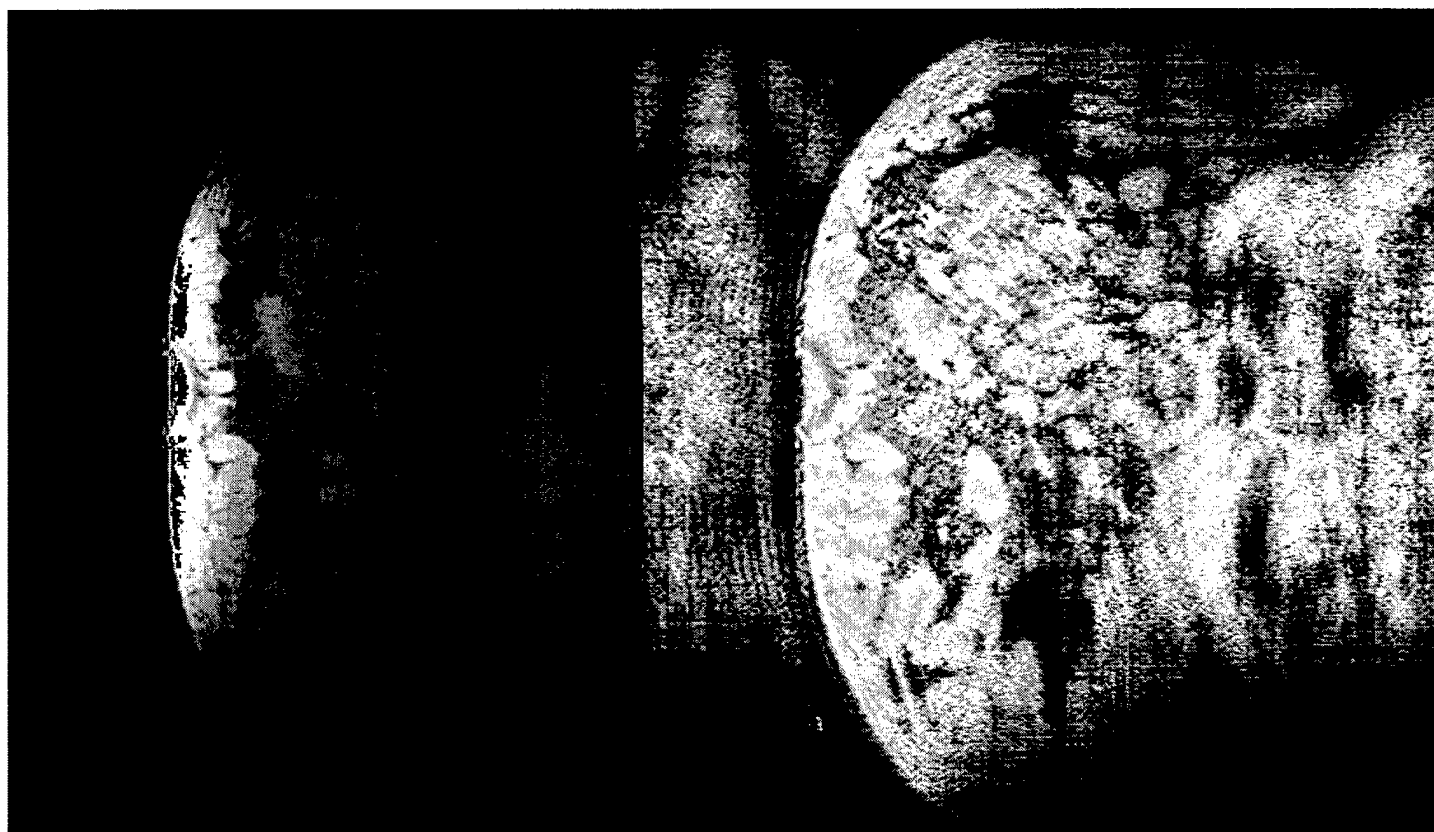


(a)



(b)

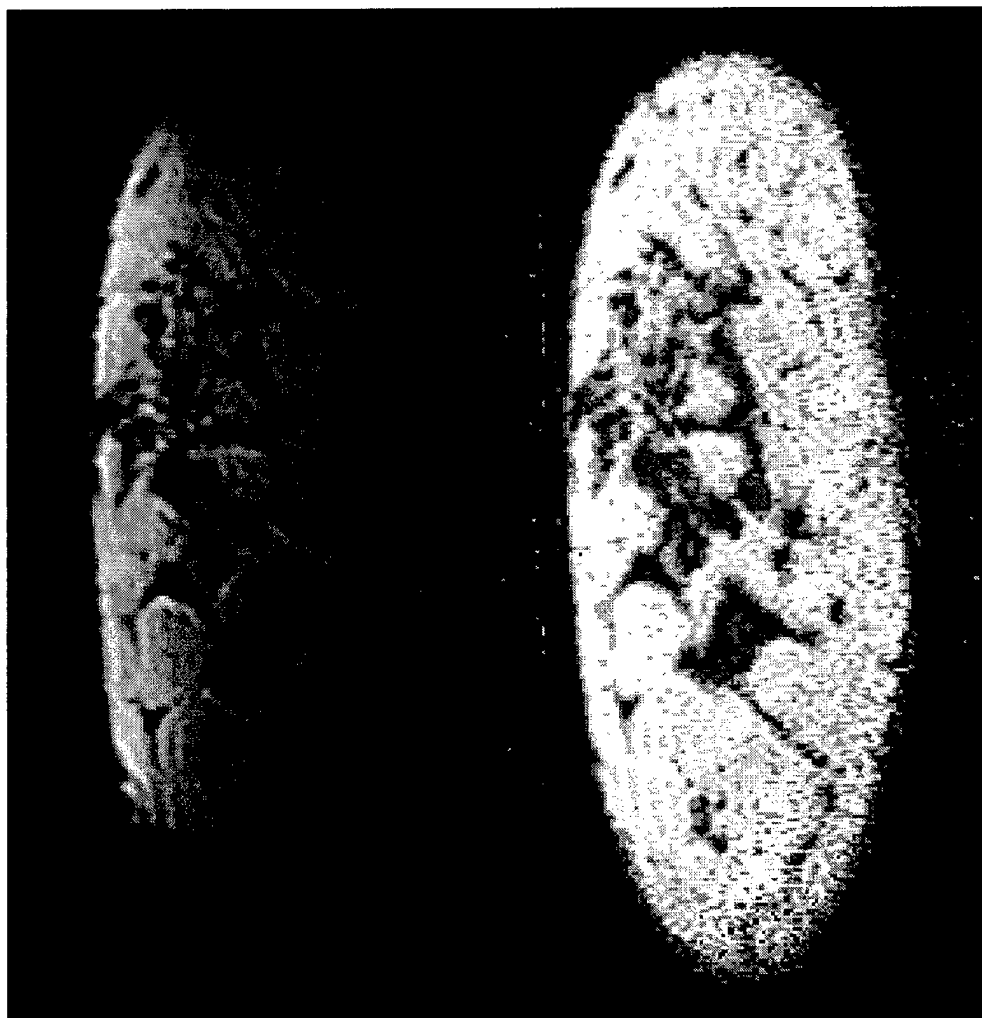
FIGURE 1. Coil and Compression device.



(a)

(b)

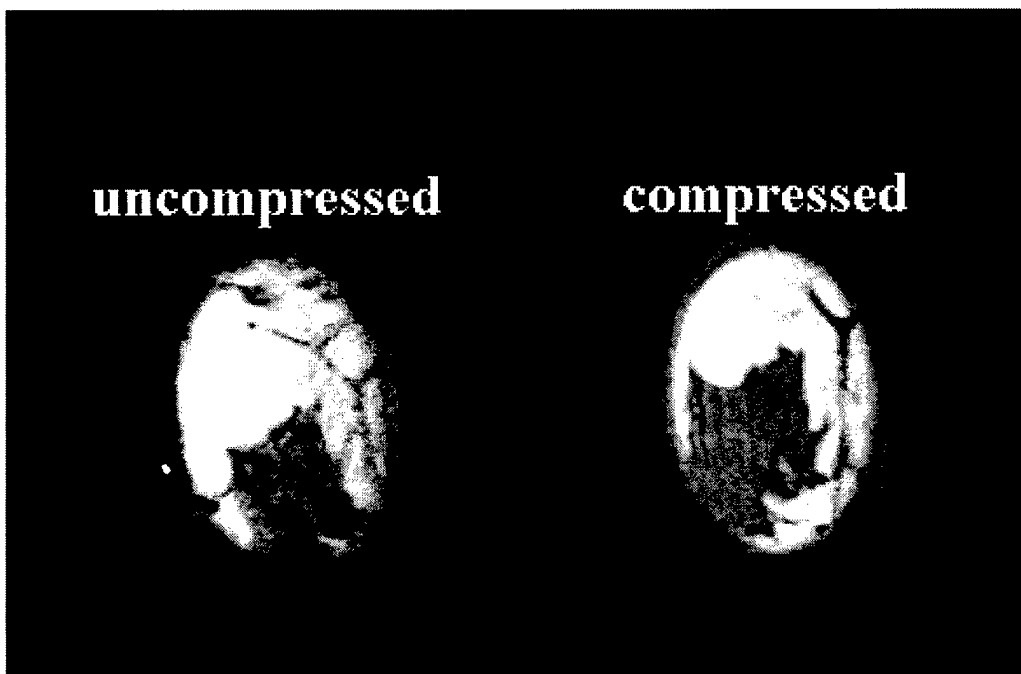
FIGURE 2. Coronal breast images illustrating filtering intensity correction algorithm.
(a) Original Image (b) Corrected image using method of reference [9].



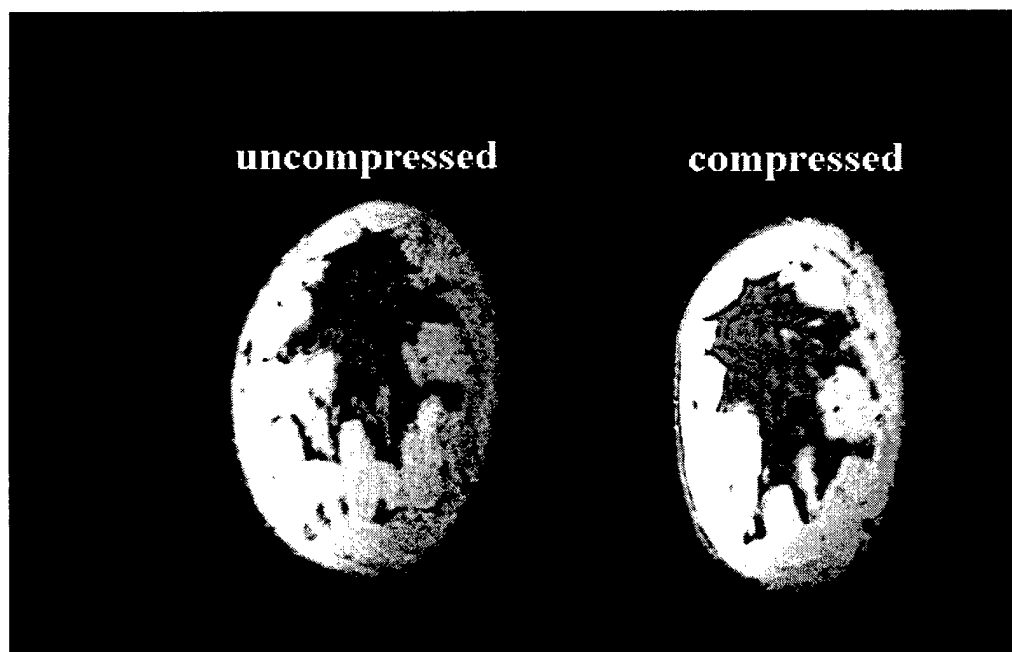
(a) Original image

(b) Intensity corrected image

FIGURE 3. Breast images resulting from new intensity correction algorithm, reference [12].



(a)



(b)

FIGURE 4. Views of mechanical deformation. (a) Sections near the nipple, (b) Sections closer to the chest wall.

(a) prone

(b) supine

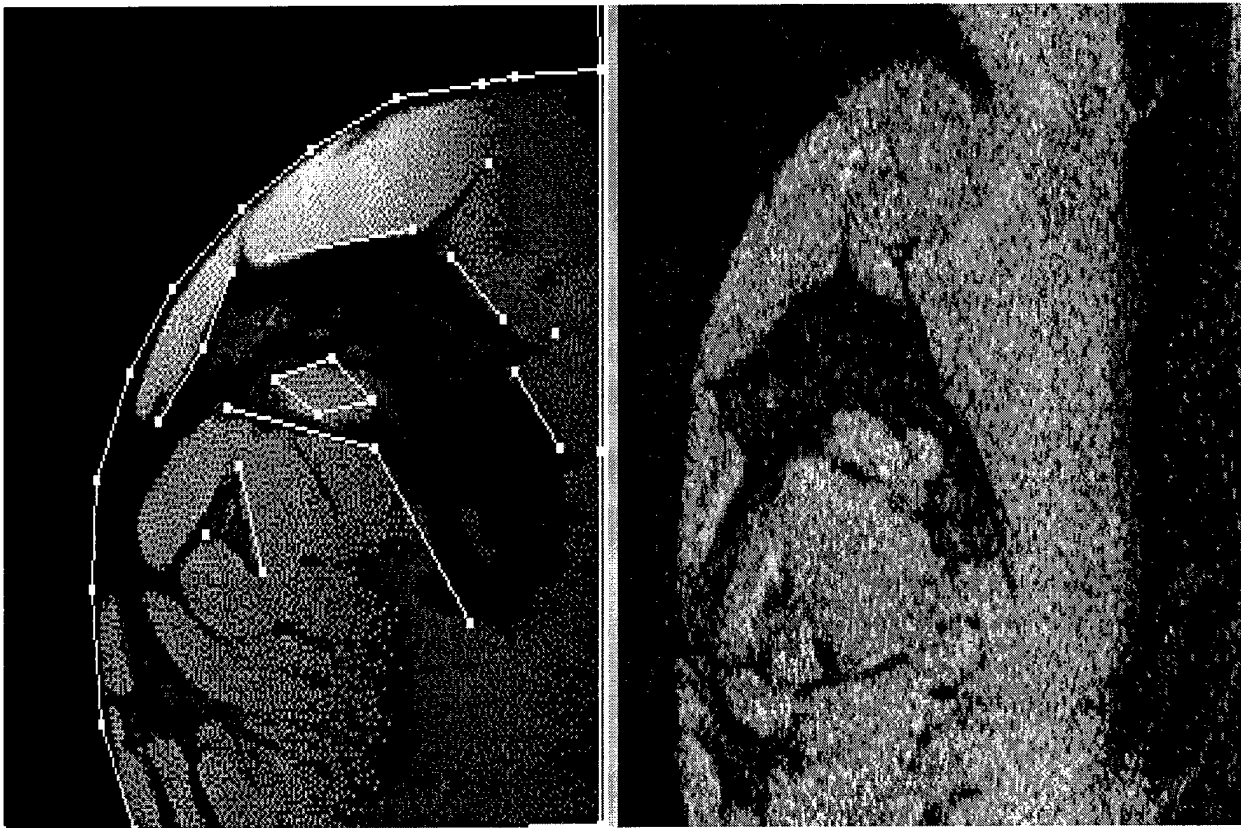
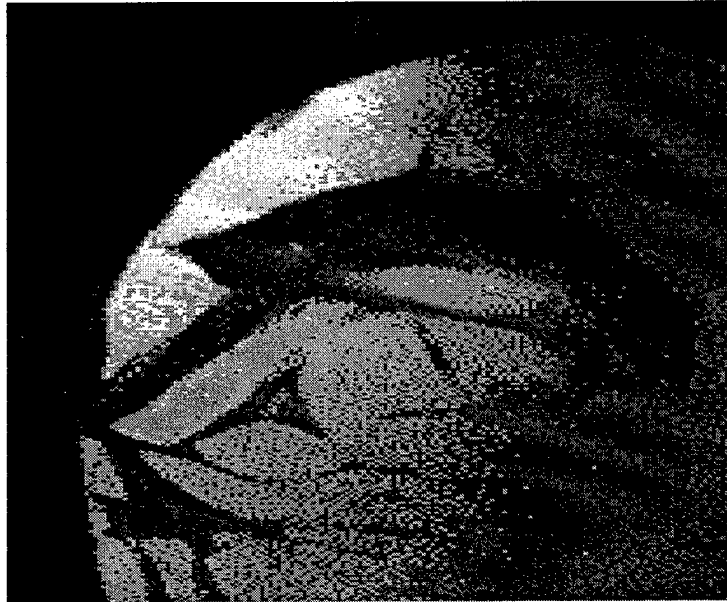
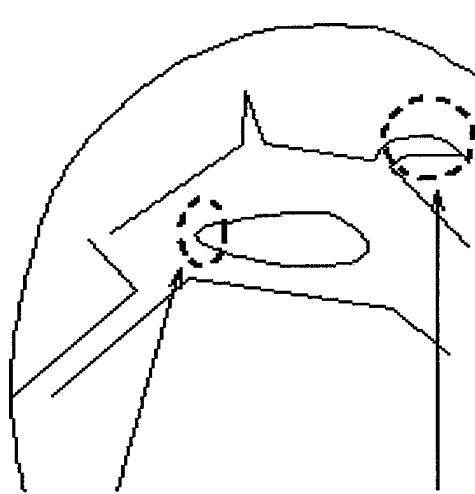


FIGURE 5. (a) Source (prone) image with identifying landmark features. (b) Target (supine) image.



(a)



(b)

FIGURE 6. (a) Morphed image resulting from feature-based morphing algorithm. (b) Incorrectly morphed areas.

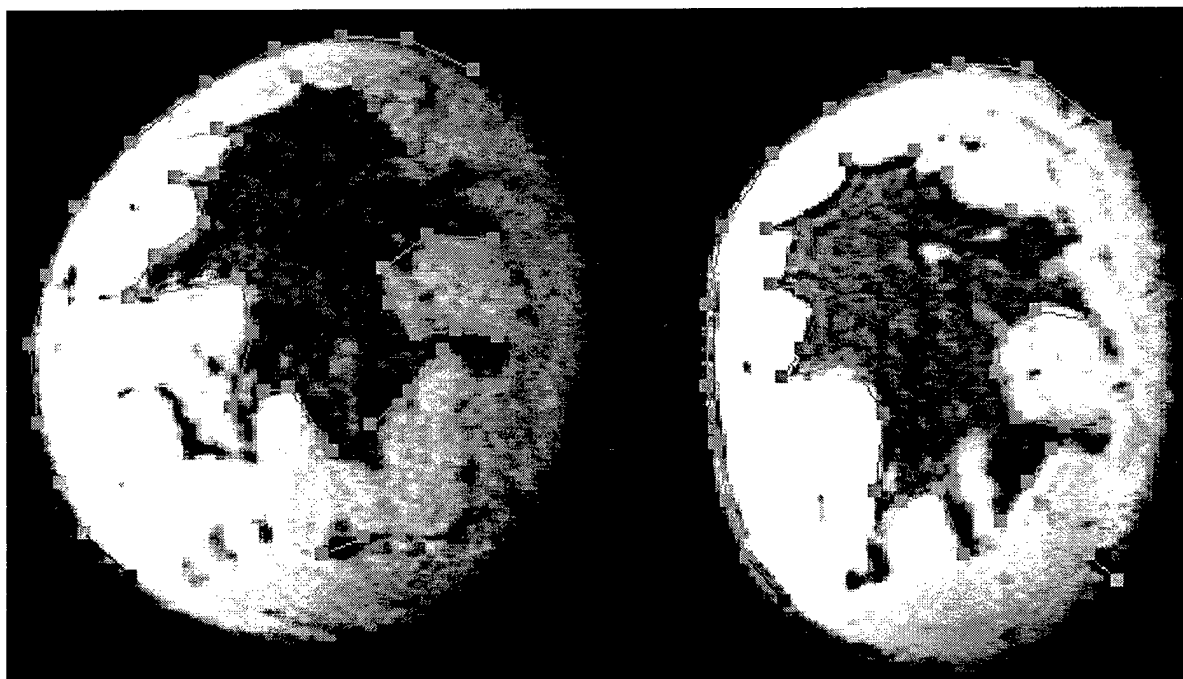


(a)



(b)

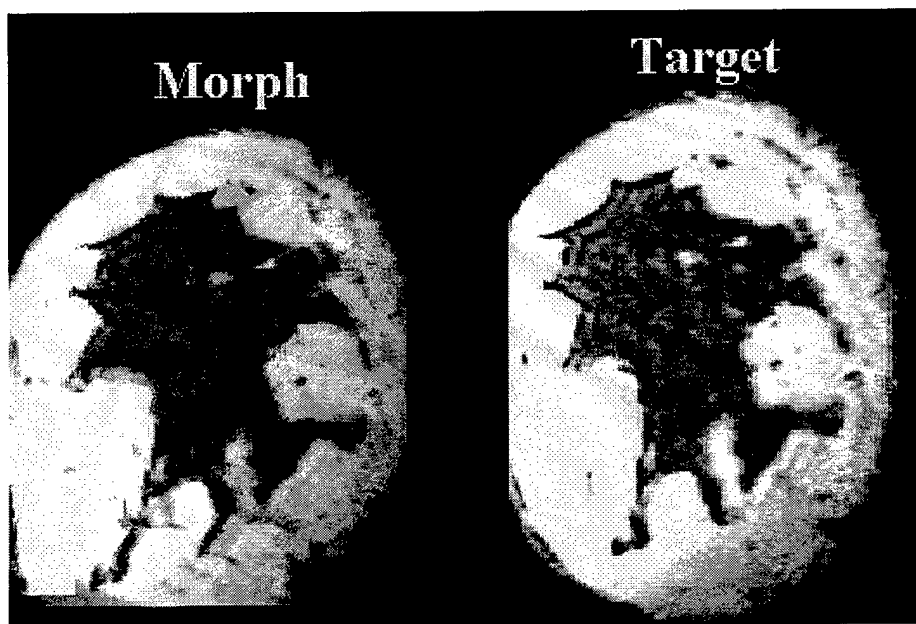
FIGURE 7. Morphs generated from (a) Feature-based, and (b) Foldover algorithms



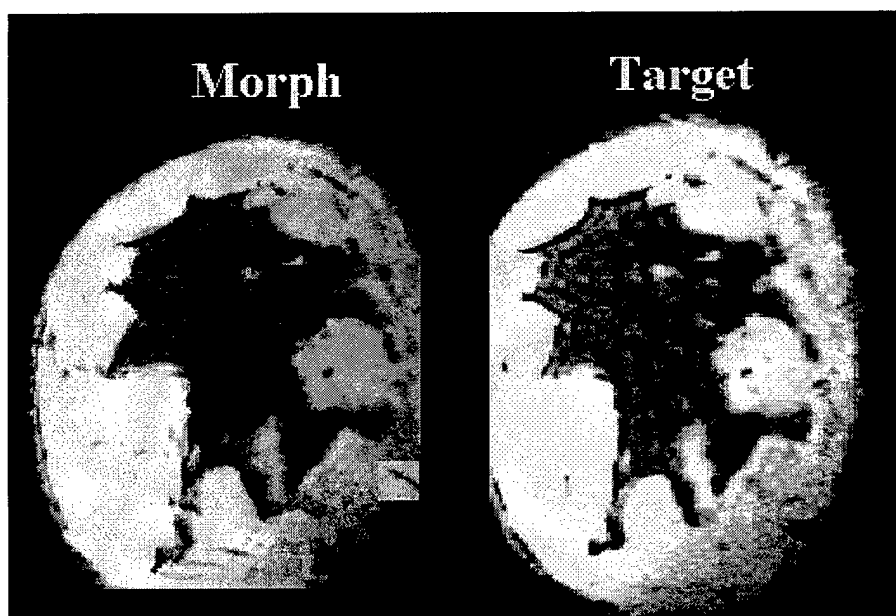
(a)

(b)

FIGURE 8. (a) Source (uncompressed) image with identifying feature control points and lines.
(b) Target image

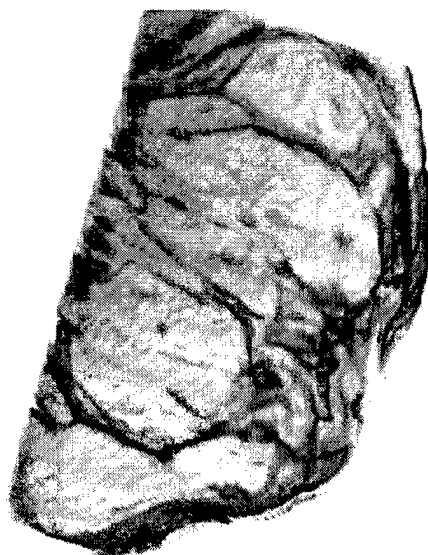


(a)

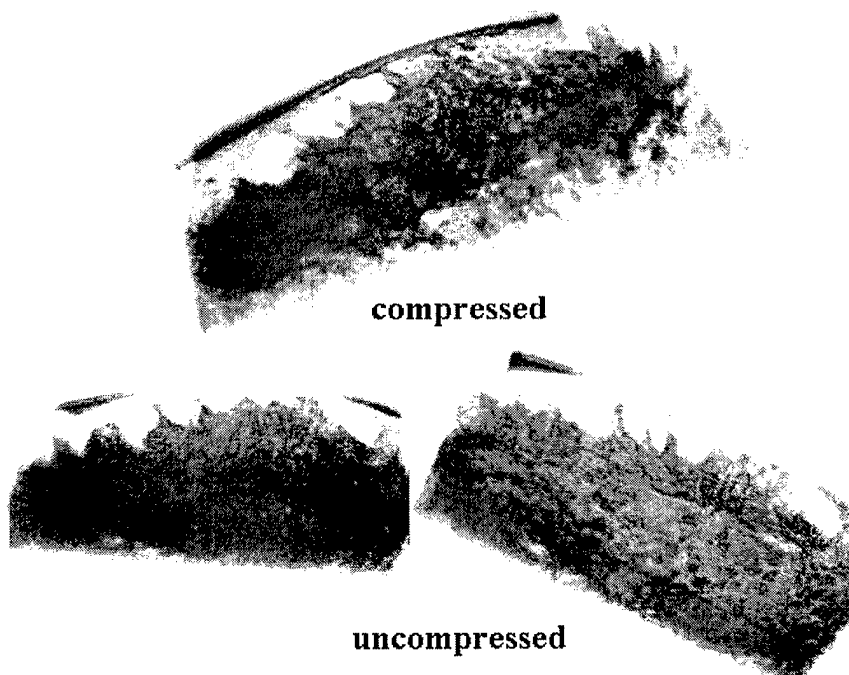


(b)

FIGURE 9. Morph images resulting from Feature based algorithms generated with (a) 20 Control Points, (b) 42 Control Points.



(a)

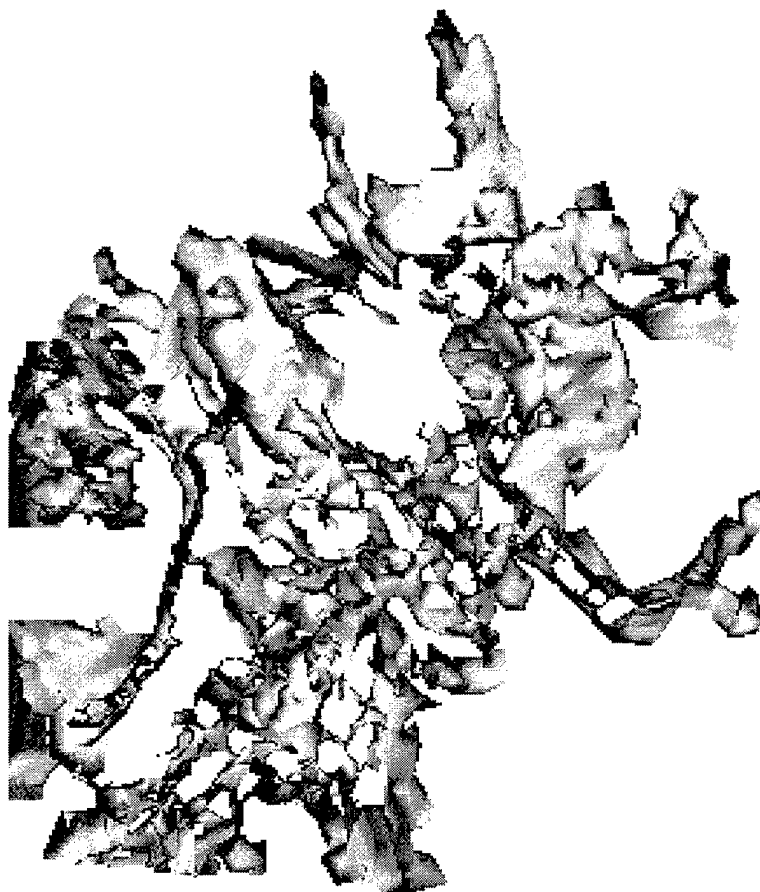


(b)

FIGURE 10. 3D renderings of MR volume data (a) Sagittal section of breast (b) Coronal sections of segmented tissue.



FIGURE 11. Segmented uncompressed tissue rendered as isosurfaces .



(a)



(b)

FIGURE 12. (a) Compressed tissue. (b) Preliminary morphing of segmented tissue (in fig.11) generated with 12 control features.

c. Presentations and Publications

Poster Presentations

Williams, C., Clymer, B., Fujimura, K., Schmalbrock, P., “Biomechanics of Breast Tissue: Preliminary study of shape deformation of normal breast tissue.” Submitted to:

Biomedical Engineering Society (BMES) 1998 Annual Meeting.

International Society for Magnetic Resonance in Medicine (ISMRM)
Sixth Scientific Meeting, 1998.

Women’s Health Conference Ohio State University, 1997.

Schmalbrock, P., Chakeres, D., Deak, G., *Williams, C.*, Clymer, B., “MR Surface Coil Image Correction Using an Integrated Positional Reference System”, submitted to Radiological Society of North America, 84th Scientific Assembly and Annual Meeting, 1998.

C. Williams⁽¹⁾, B. Clymer, PhD⁽²⁾, P. Schmalbrock, PhD⁽³⁾, K. Fujimura, PhD⁽⁴⁾,

(1) Biomedical Engineering Center, (2) Dept. of Electrical Engineering, (3) Dept. of Radiology, (4) Dept. of Computer and Information Science
The Ohio State University, Columbus, Ohio, USA

INTRODUCTION

Presently, the imaging techniques used for diagnosis and detection of breast cancer are all performed by deforming the breast from its original shape. These shape deformations result in improved diagnostic image quality, however, the biomechanical nature of breast tissue is not taken into account. This is largely due to the fact that the biomechanical behavior of breast tissue is not fully understood. Because pathology has different elastic properties than normal tissue, the characterization of the mechanical nature of tissue may provide diagnostic information [1].

An understanding of the biomechanical properties of breast tissue may be used to develop more accurate breast models. Biomechanically-based models may be used to develop computer morphing algorithms so that initial images obtained by shape deformation can be transformed into images that represent the breast in an undeformed state. Such images may better aid surgical biopsies and breast conservation procedures, as well as improve prognosis for patients.

The primary purpose of our study is to investigate the biomechanical nature of normal breast tissue, and to develop a biomechanically-driven, feature-based computer morphing algorithm which accurately mimics the shape deformation of normal and diseased breast tissue.

METHODS

Preliminary studies of shape deformation were conducted *in vivo*. The internal and external landmarks were classified from T1-weighted MR images. The landmarks served as positional markers of the deformation. The three principle types of landmarks characterized are: 1). points where two or more structures meet, 2). tips of extrusions, and 3). tangential points

RESULTS AND DISCUSSION

In Vivo Landmarks:

In the *in vivo* studies, healthy female volunteers, over the age of 18 and pre-menopausal were studied. MR images were acquired on a 1.5 T clinical MRI system (General Electric, Signa). Using a commercial phased array breast coil, prone images were obtained. A body coil was used to image in the supine position. Tissue boundaries between glandular and fatty tissue were best delineated on high resolution T1-weighted images. The anatomical features were used as landmarks to define the control points for the morphing algorithm.

2D Morphing:

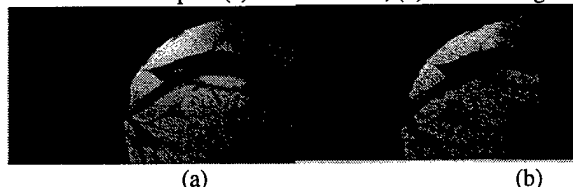
In the preliminary study, a 2D computer morphing algorithm is employed to map landmarks from the source (prone image) to the target (supine image). Image features such as points and lines, are used to guide the morphing process.

Point and line features in figure 1 are drawn at locations classified as Type 2 and 3 landmarks. The generated morphs, shown in figure 2, are less noisy than the original supine image. In figure 2a, areas of the supine image are not correctly morphed. A 2D Foldover-Free algorithm provides better one-to-one mapping, and generates a better image [2].

FIGURE 1.(a) Source and features to generate morph.(b) Target image.



FIGURE 2. Morphs (a) feature-based, (b) foldover algorithm.



3D Morphing:

MR slices were segmented with appropriate thresholding to produce the 3D image of breast tissue shown in figure 3. To perform 3D morphing, appropriate features which could be mapped to the target image were identified. Type 2 landmarks (extrusion peaks), shown in the inset, were favored. A simple morphing algorithm, known as Mesh Free Form Deformation, (MFFD), was performed and the results are shown in figure 4.

In MFFD, the object is not deformed directly, but it is embedded in a space which is deformed. The effects of deforming that space are propagated to the object. The space used to control the deformation is a 3D grid of control points. The inset depicts the morphed regions of the original object.

Methods for achieving foldover-free volume morphing are currently being studied [3]. This approach makes it possible to warp volumes seamlessly for specified feature points.

FIGURE 3. 3D representation of breast tissue. (Prone image.)

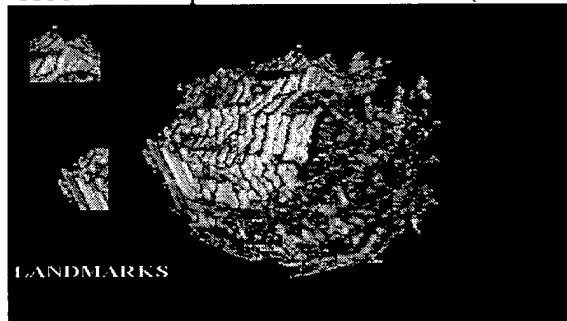


FIGURE 4. 3D morph generated with MFFD



REFERENCES

1. Porra, S., A Multimodality Approach to Breast Imaging, Aspen, Maryland, 1986.
2. Fujimura, K., Makarov, M., "Foldover-free Image Warping", to appear in SIGGRAPH December 1997.
3. Information site: www.cis.ohio-state.edu/graphics/kf

Biomechanics of Breast Tissue: Preliminary study of shape deformation of normal breast tissue.

Celeste Williams, Bradley Clymer, Petra Schmalbrock, Kikou Fujimura
Dept. of Radiology, The Ohio State University, Columbus, OH 43210

INTRODUCTION

Conventional imaging techniques used for diagnosis and detection of breast cancer are all performed by deforming the breast tissue in various ways. The shape deformation results in loss of diagnostic image quality, however the biomechanical nature of breast tissue is usually not taken into account. This is largely due to the fact that the biomechanical behavior of breast tissue is not fully understood. Because pathology has different elastic properties from healthy tissue, the characterization of the mechanical nature of breast tissue may provide improved diagnostic information [1]. An understanding of the biomechanical characteristics of breast tissue may also enhance the development of more accurate breast models.

The primary purpose of our study is to noninvasively characterize the mechanical properties of normal breast tissue, and to develop a biomechanically driven computer morphing algorithm that accurately mimics the shape deformation of normal and diseased breast tissue. In such an image analysis system, initial images obtained by shape deformation can be transformed into images of the original shape of the breast. Such an image may be used for surgical planning and breast conservation procedures, and as well as improve prognosis for patients.

METHODS

Preliminary studies of shape deformation were conducted *in vivo* using magnetic resonance imaging (MRI) on a clinical MR system (General Electric, Signa) using a surface coil designed for imaging a single breast. The breast was slightly compressed under an uniaxial compression force. The coil-compression design is shown in figure 1.

Imaging was performed with the subject lying supine with a breast between the compression plates. The breast was compressed vertically along the posterior surface of the breast, and the surface coil was attached to the bottom plate. Processing and analysis of the images were performed on a SUN UNIX system.

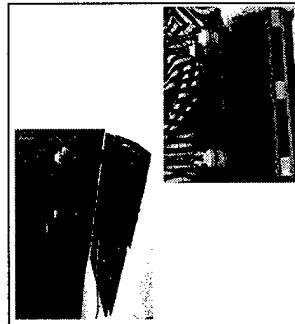


FIGURE 1. Coil and Compression device

RESULTS AND DISCUSSION

■ MRI Techniques
Images were acquired using a 3D FSPOR sequence, with a TR=25 ms, flip angle = 60°, and FOV=20x20 cm². One hundred twenty-four 1.4 mm coronal slices were obtained for each compression. The minimum compression width was 2.5 inches. Most subjects reported this compression as comfortable.

■ In Vivo Landmarks
For the *in vivo* tissue observations, healthy female volunteers over the age of 18 and pre-menopausal were studied. From preliminary imaging, anatomical features such as the rib cage, branching ducts, fatty tissue, boundaries between glandular and fatty tissue and the nipple are clearly visible. The anatomical features serve as positional markers of tissue deformation and are used as landmarks to define the control points for the morphing algorithms. The three principle types of landmarks characterized are: 1) points at which two or more structures meet, 2) tips of extrusions, and 3) tangential points along curved surfaces.

Many anatomical features were not as distinguishable on images obtained with the surface coil. Because of the inhomogeneous sensitivity profile of the coil, intensity variations masked the contrast and limited optimal display. A correction algorithm using external markers was developed to correct the surface coil images and increase tissue contrast, see figure 2.



FIGURE 2. Breast images illustrating anatomical features and initial surface coil intensity correction

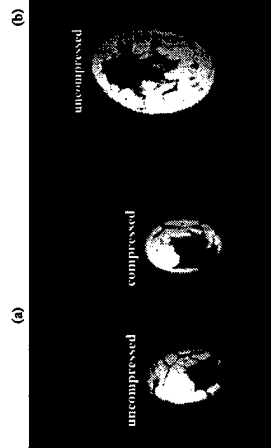


FIGURE 3. Anterior and posterior images of uncompressed and compressed breast.

■ Deformation of Breast Tissue

The mechanical behavior of breast tissue is clearly represented on the MR slices. Substantial tissue deformations are observed even under the mildest of compression. In figure 3a, above, in slices near the nipple where compression is the least, the tissue appears to have rotated. This rotation is observed in most subjects. This specific type of deformation is assumed to be associated with compression in the medial-lateral orientation. Future studies will also include craniocaudal compression. In MR slices closer to the chest wall, the correlation between anatomical features is distinguishable.

Morphing Algorithms

2D Morphing

We began our study investigating two-dimensional image processing because of the abundance of literature and available techniques in 2D morphing. Employing a 2D morphing algorithm yields a morphed image that is similar to the target image. A feature-based morphing technique known as Free Form Deformation was used to map landmarks from the source image to the target image. Each deformation is associated with a deformation parallelogram box. The points of the four corners of the box are expressed in the coordinate system of the box. The positions of the points are updated when the coordinates of the box are displaced. The defined control points and lines drive the displacement.

Image features identify the control points and lines that are used to guide the morphing process. The point and line anatomical features in figure 4a are drawn at locations classified as Type 2 and 3 landmarks. For the morphing process, the uncompressed image is the source image (e.g., the beginning of the morphing process) and the compressed image is the target, or the end of the morphing process.

Corresponding Author

Petra Schmalbrock Ph.D.
273804557
Radiology
Ohio State University College of Medicine
170 Means Hall OSU Hospital
410 West 10th Ave.
Columbus OH 43210
Phone: 6142934139 Fax: 6142936935 Ext:
Email: schmalbrock.1@osu.edu

Abstract Information

Title: MR Surface Coil Image Correction Using an Integrated Positional Reference System
Category: 9 Physics
Keyword 1: 164600 Magnetic resonance (MR), image processing
Keyword 2: 047100 Breast, MR
Keyword 3: 253670 Stereotaxis

Was this work supported by a grant from the RSNA Research and Education Fund? **No** Do you plan to submit a paper abstract on the same subject? **No**

Has this work been previously presented? **No**

Where:

Type of Exhibit: **BP**

Surface length requested (in meters): 1

More than 6 co-authors? ('et al' will appear in the program)? **No**

Number of presenting author: **1**

Co-authors

- Petra Schmalbrock Ph.D.
1 6142934139 6142936935 schmalbrock.1@osu.edu 273804557
No conflict
- Donald W Chakeres M.D.
2 6142938315 6142936935 chakeres-1@medctr.osu.edu 29620188 14424
Donald Chakeres is the inventor of the device.
- Galen Deak
3 6142675422 271821984
No conflict
- Celeste Williams BA
4 6142933045 celest@chopin.bme.ohio-state.edu 42292380
No conflict
- Brad Clymer Ph.D.
5 clymer@ee.eng.ohio-state.edu 29650 6160
No conflict
- 6
No conflict

Abstract

PURPOSE: Our goal was to create a realtime disposable MR compatible bisopy system that was simple, fast, accurate, versatile and could support multiple probes simultaneously.

METHOD/MATERIALS: We developed an integrated surface coil, breast compression plate, stereotactic pattern design with infinite vector choices, and multi-needle support system for breast biospies. The key element is a unique patented image pattern that has the characteristic that when imaged, the true distance measured between two conspicuous points is equal to the same axial dimensional distance on the device. This allows for exact immediate vector positioning and placement of the needles in targets with a expansive biopsy vector choice. We made a series of localizations on phantoms to confirm the accuracy and speed.

RESULTS: We were able to place a needles within 2 mm of the target in two minutes from the time ther were identified.

CONCLUSIONS: This type of simple accurate system could revolutionize MR bisopy techniques and lead to more definitive theraputic interventions using MRI.